Monatshefte für Chemie 117, 21—32 (1986)

Monatshefte für Chemie
Chemical Monthly

Kinetics of Thermal Decomposition of Barium Zirconyl Oxalate

T. Gangadevi, M. Subba Rao*, and T. R. Narayanan Kutty

Department of Inorganic and Physical Chemistry, Indian Institute of Science, Bangalore 560 012, India

(Received 29 June 1984. Accepted 21 January 1985)

Kinetics of the thermal decomposition of anhydrous barium zirconyl oxalate and a carbonate intermediate have been studied. Decomposition of the anhydrous oxalate, though it could be explained based on a contracting-cube model, is quite complex. Kinetics of decomposition of the intermediate carbonate $Ba_2Zr_2O_5CO_3$ is greatly influenced by thermal effects during its formation. (α-t) curves are sigmoidal and obey a power law equation followed by first order decay. Presence of carbon in the vacuum-prepared carbonate has a strong deactivating effect. Decomposition of the carbonate is accompanied by growth in particle size of the product barium zirconate.

(Keywords: Thermal decomposition; Kinetics; Barium zirconyl oxalate)

Die Kinetik der thermischen Zersetzung von Barium-zirkonyl-oxalat

Es wurde die thermische Zersetzung von wasserfreiem Barium-zirkonyl-oxalat und dem intermediären Karbonat untersucht. Die Zersetzung des wasserfreien Oxalates ist — obwohl über das „contracting-cube"-Modell erklärbar — sehr komplex. Die Kinetik der Zersetzung des intermediären Karbonates $Ba_2Zr_2O_5CO_3$ ist stark von den thermischen Effekten während seiner Bildung abhängig. Die (α-t)-Kurven gehorchen einem exponentiellen Gesetz, gefolgt von einem Zerfall erster Ordnung. Die Gegenwart von Kohlenstoff im Karbonat hat einen starken desaktivierenden Effekt. Die Zersetzung des Karbonats wird von einem Wachstum der Partikelgröße des Produktes (Bariumzirkonat) begleitet.

Introduction

Thermal decomposition of barium zirconyl oxalate heptahydrate (*BZO*) is quite complex and proceeds through a number of steps. In an earlier communication[1], it was shown that the following scheme is valid

for the thermal decomposition of *BZO*:

$$BaZrO(C_2O_4)_2 \cdot 7\,H_2O \overset{25-120\,^\circ C}{\rightleftharpoons} BaZrO(C_2O_4)_2 \cdot 2\,H_2O + 5\,H_2O \quad (1)$$

$$BaZrO(C_2O_4)_2 \cdot 2\,H_2O \xrightarrow{120-200\,^\circ C} BaZrO(C_2O_4)_2[A] + 2\,H_2O \quad (2)$$

$$2\,BaZrO(C_2O_4)_2 \xrightarrow{200-360\,^\circ C} Ba_2Zr_2O_2(C_2O_4)_{2.5}(CO_3)_{1.5} + 1.5\,CO \quad (3)$$

$$Ba_2Zr_2O_2(C_2O_4)_{2.5}(CO_3)_{1.5} \xrightarrow{360-500\,^\circ C} Ba_2Zr_2O_5CO_3[B] + 2.5\,CO + 3\,CO_2 \quad (4)$$

$$Ba_2Zr_2O_5CO_3 \xrightarrow{500-800\,^\circ C} 2\,BaZrO_3 + CO_2 \quad (5)$$

Of the various intermediates, only the anhydrous oxalate [A] and the carbonate [B] could be isolated as stable compounds. The present communication describes the kinetics of decomposition of these two intermediates.

Experimental

Materials

BZO was prepared by the interaction of freshly prepared ammonium zirconyl oxalate solution with a solution of barium acetate in the molar ratio 1 : 2 at *pH* 6[1]. Anhydrous salt [A] was obtained by heating the hydrate in air at 150 °C to constant weight. Carbonate [B] was prepared by heating *BZO* in air at 450 °C for 48 hours. A portion of this sample was aged for six months at an ambient temperature of 25 °C. Another sample of carbonate was obtained by heating *BZO* to constant weight at 450 °C in a vacuum. The three samples are designated B_1, B_2 and B_3 respectively.

Methods

Kinetic studies were conducted in a constant volume vacuum manifold which could be evacuated to 10^{-6} Torr. The volume of the system could be altered from 0.5 to 5 litres. The quantity of material taken for an experiment was such that the final pressure developed was less than 0.05 Torr. Kinetics were followed by noting the pressure increase with a *Pirani* gauge calibrated for carbon monoxide and carbon dioxide against a *McLeod* gauge. The increase in carbon monoxide pressure was used to monitor the decomposition of the anhydrous oxalate (carbon dioxide being condensed in a liquid nitrogen trap), while increase in carbon dioxide pressure was used to follow the decomposition of carbonate. Samples in the form of powders were dropped into a quartz reaction vessel maintained at the desired temperature ($\pm$ 1 °C). The final reading was taken by allowing the reaction to proceed overnight in the case of oxalate decomposition and by momentarily raising the furnace temperature by about 100 °C for the carbonate decomposition.

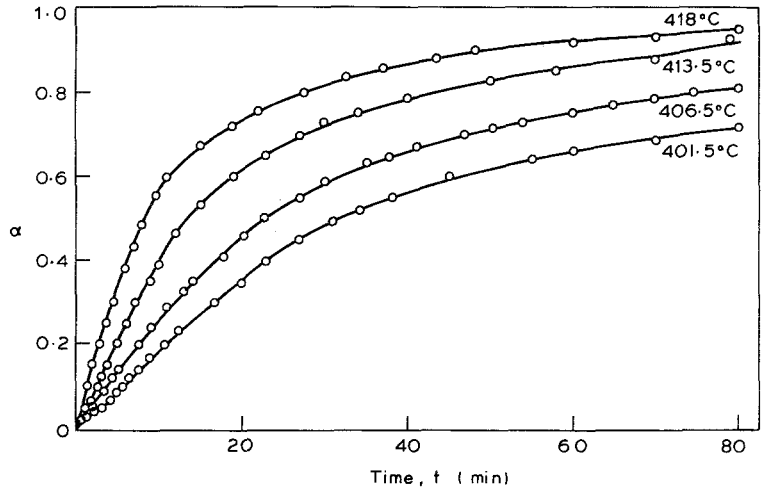

Fig. 1. (α-t) plots for anhydrous *BZO*

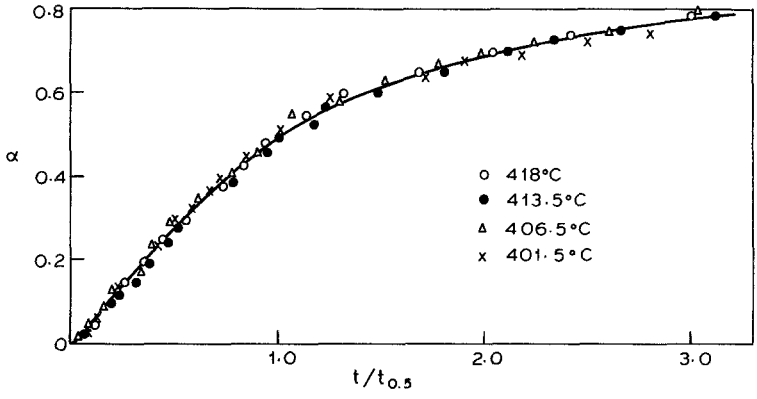

Fig. 2. α vs. $t/t_{0.5}$ plots for anhydrous *BZO*

X-ray powder diffraction patterns were recorded photographically using a Philips *Debye-Scherrer* Camera of 57.3 mm dia. and nickel-filtered copper K_α radiation from a Rich-Seifert X-ray unit.

Results and Discussion

Decomposition of the Anhydrous Oxalate

Kinetics of this decomposition were carried out in the temperature range 400–420 °C. Typical (α-t) plots at different temperatures are shown in Fig. 1. The results were reproducible and the (α-t) plots at different

temperature could be superimposed on a reduced time scale, showing that the mechanism remains the same throughout. Both the (α-t) plots and (α-$t/t_{0.5}$) plots (Fig. 2) indicate that the decomposition is deceleratory throughout. Among the various deceleratory equations, only the contracting cube equation was found to give a satisfactory fit (Fig. 3). The plots consists of two linear regions with slightly different slopes. Activation energies evaluated from the *Arrhenius* plots are 194 and 151 kJ mol^{-1} respectively. A good fit with the *Arrhenius* equation is not always proof of the validity of any isothermal kinetic equation. Analysis of kinetic data at constant α (say 0.5 α or any other definite fraction) rather than at constant "t", is a general method which will give a value of E_a (activation energy) where α is a function of (kt). Activation energy obtained by plotting log $t_{0.5}$ vs. $1/T$, shown in Fig. 4 c, is 316 kJ mol^{-1}. This is a high value and is indicative of the composite nature of the decomposition. The decomposition of the oxalate is a multistep process and both carbon monoxide and carbon dioxide are evolved simultaneously, in this temperature range. It is quite unlikely that the rates of evolution of these two gases will be the same throughout. In addition disproportionation of carbon monoxide results in the formation of carbon, which could affect the kinetics. The contracting cube model to which the kinetic data are found to fit well, is perhaps an oversimplification of an inherently complex deceleratory kinetics.

Decomposition of the Intermediate Carbonate, $Ba_2Zr_2O_5CO_3$

Unlike the anhydrous oxalate which was amorphous to X-rays, the carbonate is reasonably crystalline and gives a distinct X-ray diffraction pattern. Analysis of the pattern indicated this to be a distinct phase and not a mixture of barium carbonate, zirconium dioxide and barium zirconate.

Samples B_1 and B_2 are white flowing powders, whereas B_3 is black owing to the presence of elemental carbon deposited during its preparation. Kinetics of decomposition of the three samples show differences both in the temperature range of their decomposition and the magnitude of the activation energies. The detailed kinetic results are presented in Table 1.

Typical (α-t) plots for B_1, B_2 and B_3 are shown in Figs. 5, 6, and 7 respectively. A reduced time plot of the same data is presented in Fig. 8. The plots of Fig. 8 do not overlap, indicating that the three samples decompose by different mechanisms. All the (α-t) plots are sigmoidal and do not exhibit any induction period. For B_1 and B_2, the acceleratory periods are short with inflection points around 0.2 α. For sample B_3, the

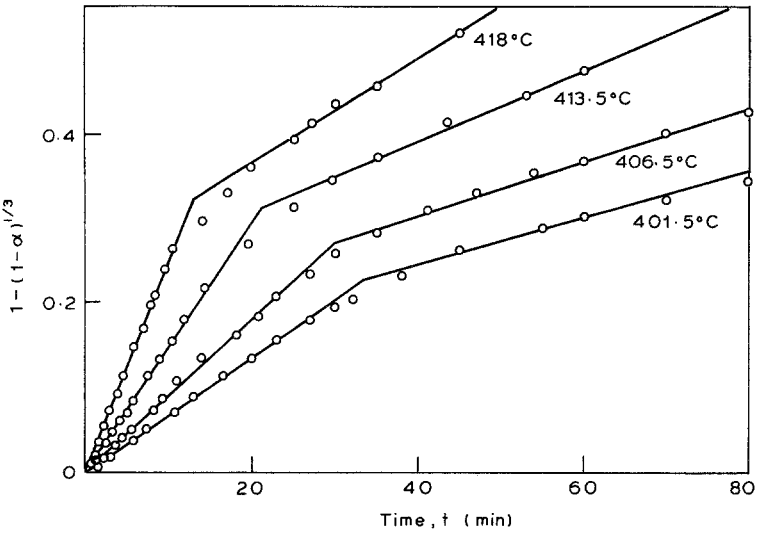

Fig. 3. 1-(1-α)$^{1/3}$ vs. t plots for anhydrous *BZO*

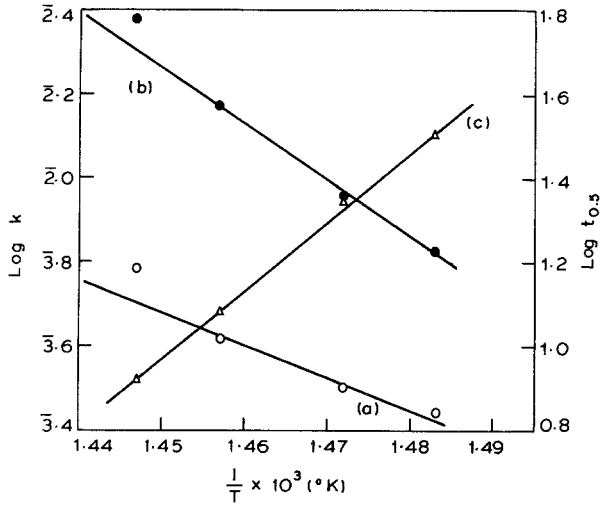

Fig. 4. (a) and (b) *Arrhenius* plots for anhydrous *BZO*; (c) log $t_{0.5}$ vs. $1/T$ plot for anhydrous *BZO*

Table 1. *Results of the kinetics of decomposition of the carbonate B*

Sample	Temp. range of decomposition in K	α_i	Equation obeyed		Activation energy kJ mol^{-1}	
			Acceler-atory	Decay	Acceler-ation	Decay
B_1	873–908	0.20	$\alpha = (kt)^2$	$-\log(1-\alpha) = kt$	207	228
		0.40		$\log\frac{\alpha}{1-\alpha} = kt$	230	259
B_2	823–843	0.20	$\alpha = (kt)^2$	$-\log(1-\alpha) = kt$	197	195
		0.60		$\log\frac{\alpha}{1-\alpha} = kt$	191	176
B_3	978–1 003	0.50	$\alpha = k^3(t-t_0)^3$	$-\log(1-\alpha) = kt$	722	643
		$0.1 < \alpha < 0.9$		$\log\frac{\alpha}{1-\alpha} = kt$	800	

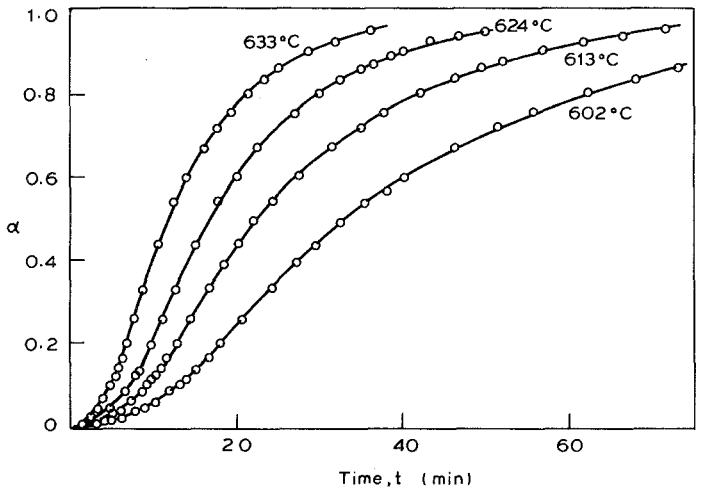

Fig. 5. (α-t) plots for B_1

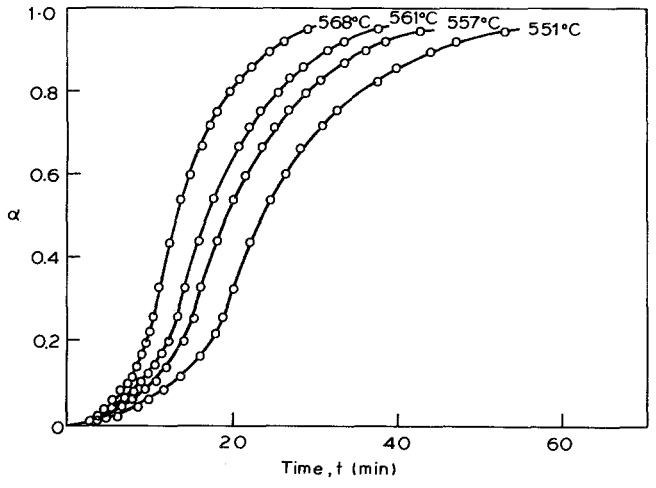

Fig. 6. (α-t) plots for B_2

acceleratory period is more pronounced with the inflection point around 0.5 α. The differences in the kinetic behaviour of the samples can be explained on the basis of the conditions prevailing during their preparation.

During the formation of B_1, it is subjected to self-heating owing to the exothermic nature of the oxalate decomposition in air. This might cause

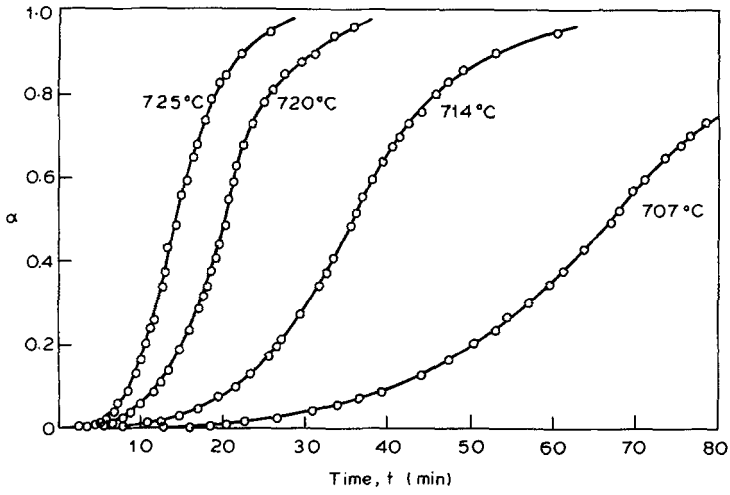

Fig. 7. (α-t) plots for B_3

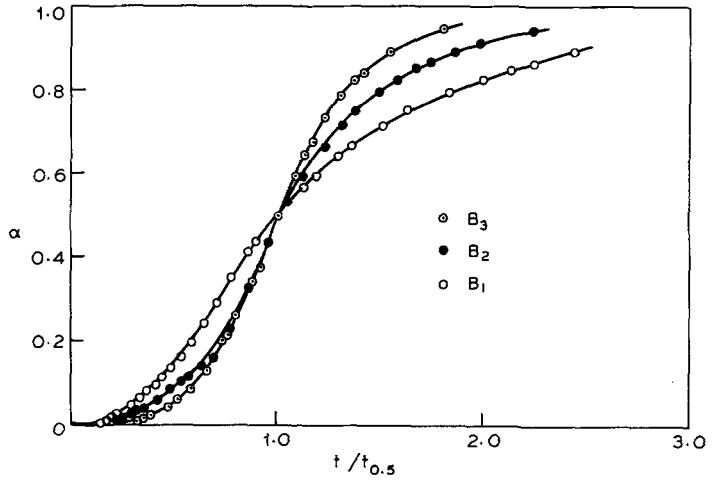

Fig. 8. α vs. $t/t_{0.5}$ plots for B_1, B_2, and B_3

further decomposition of the carbonate at preferential sites giving rise to the nuclei of the product, barium zirconate. In addition the sample is subjected to a considerable thermal strain during its preparation, which would facilitate the formation of a large number of product nuclei. The acceleratory period up to α_i is described by the power law equation, $\alpha = (kt)^2$. Obedience to square law is possible in either of two cases:

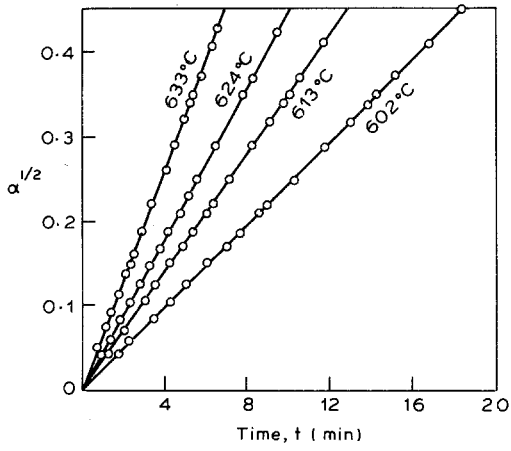

Fig. 9. $\alpha^{\frac{1}{2}}$ vs. t plots for B_1

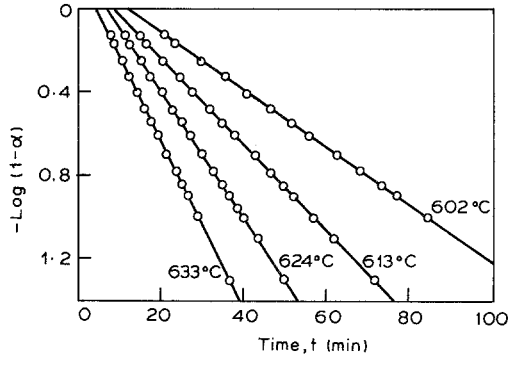

Fig. 10. First-order plots for B_1

instantaneous nucleation followed by two dimensional growth or a single step nucleation followed by linear growth. The latter is not preferred since it is already indicated that growth nuclei are present in the sample. The constancy of α_i and its low value implies the presence of a constant but large number of nuclei, which impinge on one another at a low value of α. This results in a pronounced decay period, which obeys the first-order law. For this to be valid, either of two situations should prevail[2]: (a) the earlier decomposition may result in an exponential distribution of completely nucleated particles; (b) as a result of the separation of the reactant matrix during the acceleratory period, a large number of precisely equivalent particles containing no growth nuclei is formed; each particle is

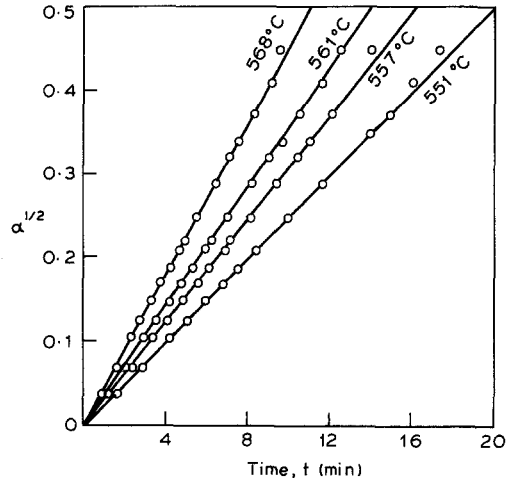

Fig. 11. $\alpha^{\frac{1}{2}}$ vs. t plots for B_2

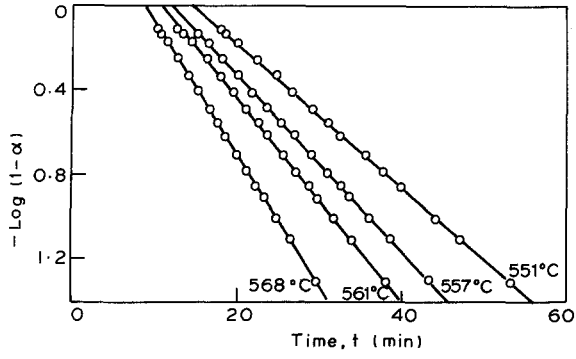

Fig. 12. First-order plots for B_2

activated individually and then decomposes. The decomposition of the carbonate is accompanied by particle growth, as shown by distinct crystallinity of the product, barium zirconate. This indicates a coherence of the reactant-product interface, which would not favour the possibility (b). The activation energies for the acceleratory and decelerator periods are 207 kJ mol^{-1} and 228 kJ mol^{-1}. These are of the same magnitude as values reported for similar decompositions. The aged sample B_2 obeys the same kinetic laws as B_1. However there is both a lowering of decomposition temperature as well as activation energies (197 and 195 kJ mol^{-1}). This is possibly due to the ordering of growth nuclei, during ageing. Kinetic data on the samples B_1 and B_2 could also be analysed on

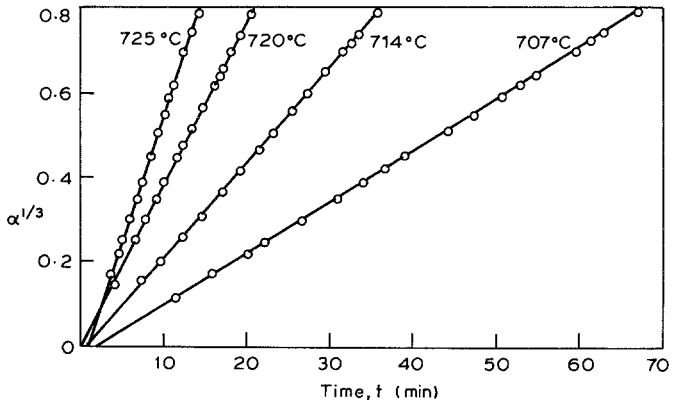

Fig. 13. $\alpha^{1/3}$ vs. t plots for B_3

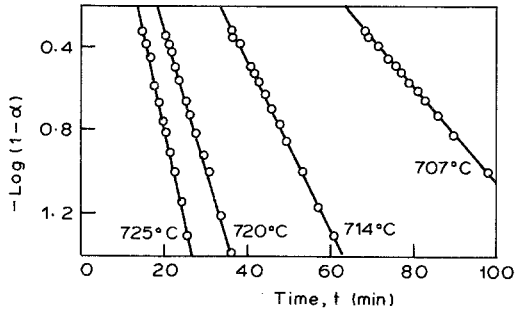

Fig. 14. First-order plots for B_3

the basis of the *Prout-Tompkin* equation. The activation energies are of the same magnitude as the previous analysis. But the values of α_i are quite high which would indicate a small number of initial nuclei. However the conditions of preparation of the samples B_1 and B_2 favour the formation of a large number of growth nuclei and consequently overlap of nuclei at a low value of α.

B_3 has an entirely different thermal history, owing to the endothermic nature of oxalate decomposition in a vacuum. There is self-cooling which is not conducive to the formation of growth nuclei, during the preparation of B_3. In addition, elemental carbon which is produced by the disproportionation of carbon monoxide: $2\,CO \rightarrow CO_2 + C$, gets deposited on the sample. This deposit is likely to occur preferentially at active sites such as points of emergence of dislocations at the surface[3]. This results in

deactivation of potential nucleus forming sites. Additionally carbon deposit can inhibit the escape of carbon dioxide. Hence the decomposition temperature would be higher and the activation energies will also be higher (722 and 643 kJ mol^{-1}). B_3 obeys a cubic law (Fig. 13) in the acceleratory period, which can be explained as due to a single step nucleation followed by two-dimensional growth. The raising of the inflection point to $0.5\,\alpha$ indicates the number of nuclei to be relatively

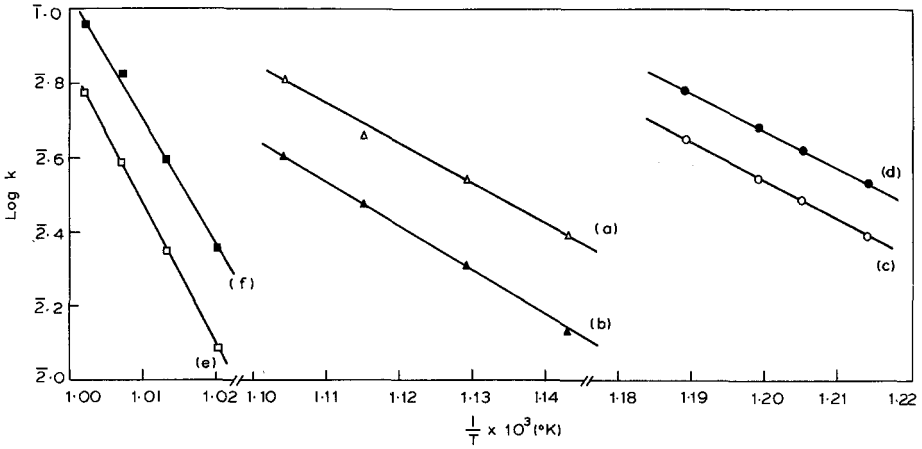

Fig. 15. *Arrhenius* plots: (a) and (b) B_1; (c) and (d) B_2; (e) and (f) B_3

small. The decay period obeys the first-order law (Fig. 14) in line with B_1. Here again the *Pront-Tompkin* equation is found to give a good fit in the entire range $0.1 < \alpha < 0.9$. However, conditions favourable for branching of nuclei (assumed in the derivation of *Pront-Tompkin*'s equation) are absent, since most active sites and dislocation channels are blocked by carbon deposit. Hence the fit of the kinetic data to the *Pront-Tompkin* equation is just fortuitous.

Acknowledgements

One of us (*TG*) is grateful to the Council of Scientific and Industrial Research, India, for the award of a research fellowship.

References

[1] *Gangadevi T., Subba Rao M., Narayanan Kutty T. R.*, J. Thermal Anal. **19**, 321 (1980).
[2] *Young D. A.*, Decomposition of Solids, pp. 52. Oxford: Pergamon Press. 1966.
[3] *Thomas J. M.*, Adv. Catalysis Vol. 19, p. 348. New York: Academic Press. 1969.